Contents lists available at ScienceDirect

Urban Climate

journal homepage: www.elsevier.com

Numerical characterization of spatial and temporal evolution of summer urban heat island intensity in São Paulo, Brazil

Arissa Sary Umezaki [a], Flavia Noronha Dutra Ribeiro [a,*], Amauri Pereira de Oliveira [b], Jacyra Soares [b], Regina Maura de Miranda [a]

[a] School of Arts, Sciences and Humanities - University of Sao Paulo, Av. Arlindo Bettio, 1000 Vila Guaraciara, Sao Paulo, SP CEP: 03828-000, Brazil

[b] Institute of Astronomy, Geophysics and Atmospheric Sciences - University of Sao Paulo, Rua do Matao, 1226, Cidade Universitária, São Paulo, SP CEP: 05508-090, Brazil

ARTICLE INFO

Keywords:
Urban climate
Urban heat island
Sea breeze
Cold fronts
WRF model

ABSTRACT

The WRF model was used to simulate the air temperature field in January in São Paulo, Brazil, for 10 consecutive years (2004–2013), and to estimate the intensity of the urban heat island (UHI). The analysis considered: days with sea breeze passages, days with cold fronts, days with no sea breeze or cold front passages, and all days. The UHI intensity varied from 1.5 to 2.5 K between 0000 local time (LT) and 1100 LT, and from 2.5 to 3.5 K between 1200 LT and 2300 LT. The UHI core was aligned in the SW-NE direction during daytime. At night, the UHI core was larger, expanding over the urban area. The synoptic conditions substantially impacted the UHI intensity, spatial variability, and diurnal pattern: sea breeze days presented the highest UHI intensity and amplitude during the day; cold front days presented the smallest amplitude of UHI diurnal variability; and days with no fronts presented a larger area of higher temperatures, particularly at night. The UHI intensity for January 2014 was compared to the 10-year average for January. It presented a higher UHI intensity at night than the average for January and showed a UHI diurnal pattern similar to the sea breeze pattern.

1. Introduction

Today, more than half of the world population lives in urban areas. Thus, it is imperative to understand how the urbanization impacts local weather and climate, to better plan mitigation and adaption measures (Grimmond, 2007). For example, extreme heat events increase morbidity and mortality rates in cities worldwide (Harlan and Ruddell, 2011). A transition in urban infrastructure, energy consumption, and land use is needed to limit global warming under 1.5 °C until 2100 (de Coninck et al., 2018).

The Metropolitan Region of São Paulo (MRSP), a conurbation of 39 municipalities, is the largest such region in South America, and is home to more than 20 million people. Its large area (approximately 8000 km^2) and diversity of land use (highly populated residential and commercial areas, urban parks, protected vegetated areas, agricultural areas, and water bodies) creates a challenging site for studying urban influences on atmospheric conditions (Fig. 1). Additionally, it is located in a terrain with a complex topography (Fig. 1b), in a plateau NW from an escarpment that separates the metropolitan area from the coastline (Oliveira et al., 2003; Ribeiro et al., 2018). In São Paulo, one of the impacts of the urban heat island (UHI) concerns flooding events; the convergence

* Corresponding author.
E-mail address: flaviaribeiro@usp.br (F.N.D. Ribeiro)

https://doi.org/10.1016/j.uclim.2020.100615
Received 30 April 2019; Received in revised form 25 January 2020; Accepted 12 March 2020
Available online xxx
2212-0955/

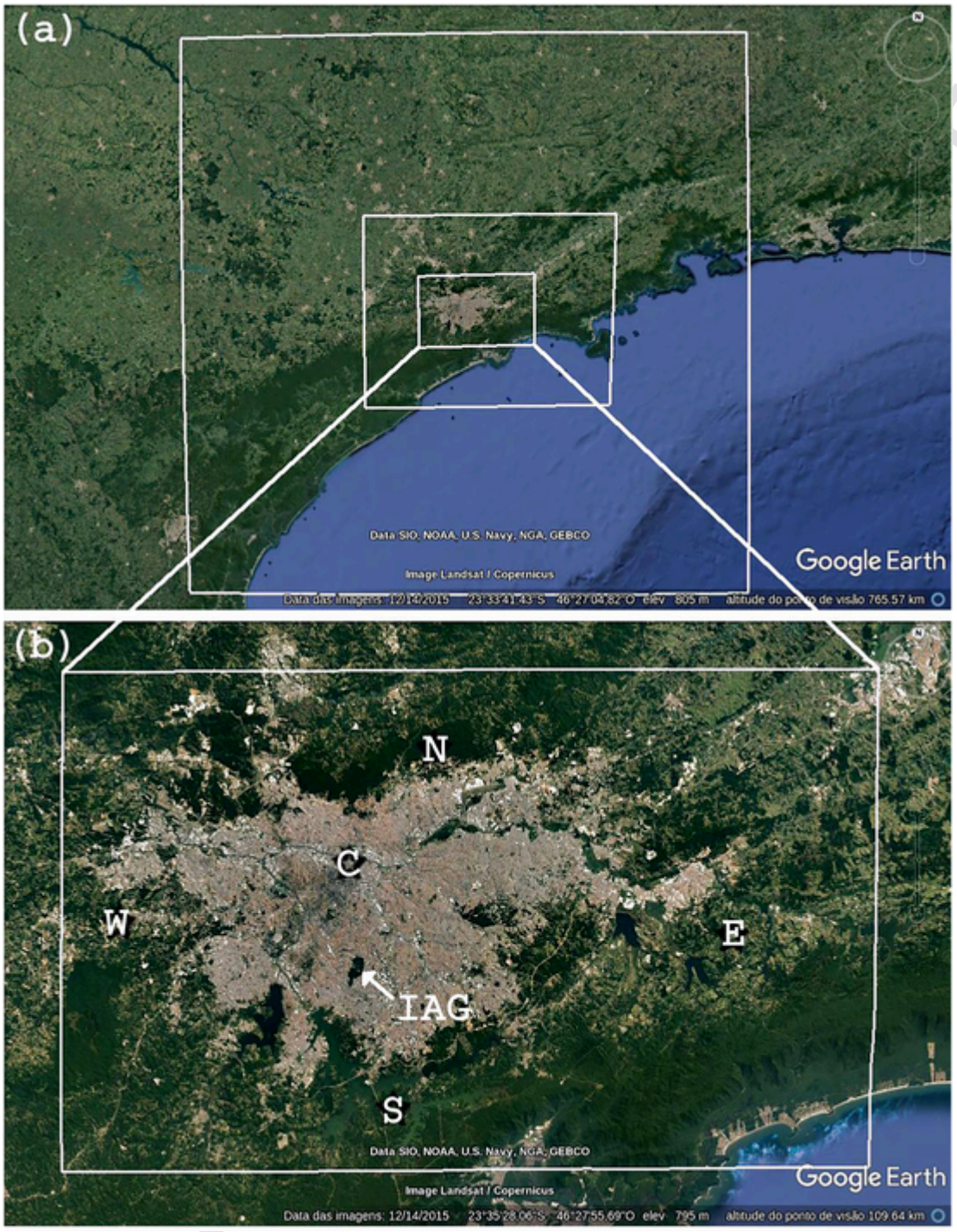

Fig. 1. (a) The study area and the numerical model domains (white rectangles). (b) The innermost domain (white rectangle), comprising most of the Metropolitan Region of Sao Paulo, and the location of the IAG surface meteorological station (white arrow), the urban center ('C'), and the rural points at the north ('N'), the south ('S'), the west ('W'), and the east ('E') of the urban area.

caused by the interaction between a sea breeze (SB) front and the UHI flow, under pre-frontal northwestern flow conditions, causes severe precipitation (Vemado and Pereira Filho, 2016).

Ferreira et al. (2012) evaluated the UHI intensity in the MRSP in 2004 using surface station data, and showed a maximum UHI intensity of approximately 5.5 °C during spring, from 1300 local time (LT) to 1600 LT. Additionally, an urban cold island was observed during winter, from 0800 LT to 1000 LT. To estimate the UHI intensity, the authors used the hourly differences between the

average temperatures of six rural stations and nine urban stations for the year 2004. However, the rural stations were all located southeast from the urban area. As the SB comes from the southeast, the estimated UHI intensity is highly impacted by this circulation. This was demonstrated by Ribeiro et al. (2018), who used numerical simulations to compare the temperature differences calculated between an urban point and two rural points, one located south from the city and another north from the city, during a SB front passage. Silva et al. (2017) performed a statistical analysis of surface station data from 2002 to 2011. The temporal analysis presented a diurnal pattern similar to the one calculated by Ferreira et al. (2012), and a seasonal pattern, with spring recording the highest and lowest UHI values. These patterns were related to the degree of urbanization and wind flow. A cluster analysis indicated six groups of similar temperature patterns. They used data from nine surface stations, all located inside the urban area. Their work highlights the substantial spatial variability of the temperature field within the city, and also suggests the influence of SBs on UHI intensity. Barros and Lombardo (2016) used satellite data to compare the surface UHI and leaf index area, and found surface temperature differences up to 8 °C. As their study aimed to relate the surface temperature to the presence of vegetation, they used satellite images for one day (09/28/2011), providing a picture of the contribution of surface characteristics to UHI intensity. Together, these works address parts of the UHI pattern in São Paulo, but a more comprehensive investigation is lacking. Therefore, a numerical study performing long-term simulations may help fill the gaps regarding the average spatial structure of the UHI.

Local and larger-scale circulations often disturb weather conditions in the MRSP, advecting air with different characteristics, and changing the temperature field and the UHI intensity (Dias and Machado, 1997; Freitas et al., 2007; Ribeiro et al., 2018). The presence of the escarpment south from the MRSP and the proximity to the coast favor the propagation of SB fronts. Once developed at the coast, the SB couples with the mountain-valley circulation and flows up the escarpment, reaching the plateau. However, northwesterly wind speeds ranging from 7 to 10 m s^{-1} prevent the SB front from reaching the urban area (Bischoff-Gauß et al., 1998; Dias and Machado, 1997). The UHI may cause a thermal circulation, with surface flow converging towards the city center, updrafts over the center, diverging flow in altitude, and down-drafts outside the urban area (Hidalgo et al., 2010). When the SB front reaches the city, it is accelerated towards the city center and decelerates after it, owing to the opposing branch of the UHI circulation, and the UHI center may be shifted (Ackerman, 1985; Chemel and Sokhi, 2012; Keeler and Kristovich, 2012; Kusaka et al., 2000; Yoshikado, 1992). These effects were also noticed in the MRSP (Ribeiro et al., 2018).

In the summer of 2014, an anomalous high-pressure center developed in the low and medium levels of the atmosphere over the southeast region of Brazil. This high-pressure center caused subsidence, inhibiting cloud formation and decreasing air humidity. Additionally, it blocked the passage of cold fronts (CFs) and the advection of humidity from the Amazon, thus preventing the formation of the South Atlantic convergence zone (Marengo et al., 2015). These conditions persisted for 45 days, starting in the beginning of January. As a result, the hotter and drier conditions caused a drought in São Paulo. The MRSP suffered from water supply restrictions and excessive heat. The Institute of Astronomy, Geophysics and Atmospheric Sciences (IAG) surface station (Fig. 1b) recorded the second-highest maximum temperature and the second-highest number of hours of clear skies for the month of January (IAG-USP Meteorological Station, 2014).

Ribeiro et al. (2015), motivated by the extreme heat observed during January 2014, used observational data from three surface stations (one urban station and two suburban stations) to calculate a ten-year average (2004 to 2013) of the UHI intensity during summer, and compared it to the average UHI intensity in 2014 to investigate the implications of the anomalous conditions on the UHI intensity. In January 2014, the UHI was 1 to 2 °C higher than the ten-year average, suggesting that the anomalous conditions also increased the UHI intensity. In December 2013 and February 2014, the UHI intensity was closer to the average. However, the three surface stations used by Ribeiro et al. (2015) did not provide sufficient information to represent the spatial variability of the air temperature field over the MRSP. The lack of observational data is addressed herein, by using a numerical model. To further understand the characteristics of the UHI phenomenon in São Paulo, the present work aims to determine the average UHI spatial and temporal patterns in São Paulo during January, to investigate how mesoscale and synoptic conditions contribute to these patterns, and to determine how anomalous the January 2014 UHI pattern was.

2. Material and methods

This section describes the study area, and the set of numerical simulations.

2.1. Study area

The MRSP (Fig. 1) is located approximately 50 km from the coast, in a plateau 700 m above the mean sea level. The terrain is complex, with a mountain range limiting the urban expansion in the north direction, and a massif escarpment at the west. The escarpment, southeast from the city towards the coast, also complicates the topography of the area. Moreover, there are many small elevations and river valleys inside the urban area. The climatological means recorded at the IAG station for January from 1933 to 2014 are: temperature of 21.6 °C, precipitation of 231.9 mm, and relative humidity of 82.5%. The predominant wind direction is from the SE, owing to the frequent propagation of SB fronts (IAG-USP Meteorological Station, 2014), which reach the urban area 50% of the days of the year (Perez and Silva Dias, 2017). CFs regularly propagate over the city, arriving from the SW direction (Oliveira et al., 2003), increasing cloudiness and precipitation, and decreasing air temperature. Fig. 2a and b show an example of a typical pattern for summer: a high-level cyclonic vortex is located over the Atlantic Ocean, near the northeast of Brazil (Fig. 2a), and the South Atlantic convergence zone is over the southeast (light green-striped zone, Fig. 2b), causing precipitation.

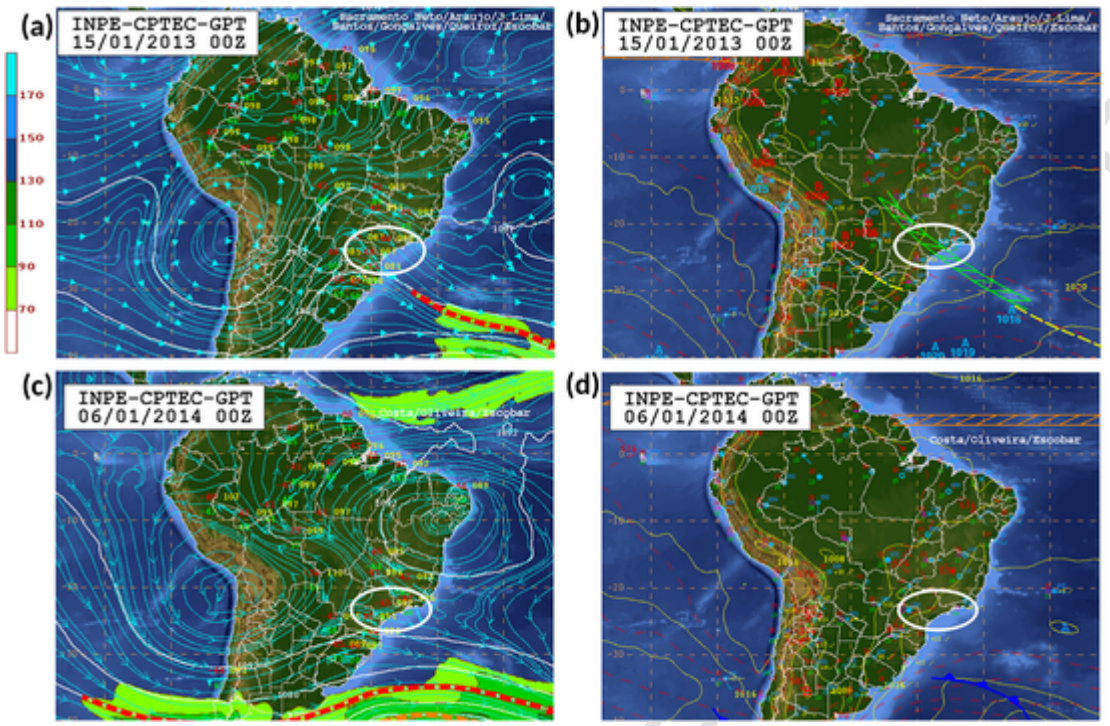

Fig. 2. Synoptic charts on 15 Jan 2013 at (a) 250 hPa and (b) the surface and on 6 Jan 2014 (c) 250 hPa and (d) the surface, provided by the Brazilian Center for Weather Forecast and Climate Studies of the National Institute of Space Research (CPTEC-INPE, available on line at http://tempo.cptec.inpe.br/boletimtecnico/pt). White ellipsis highlights the Sao Paulo state location.

2.1.1. The summer of 2014

In January 2014, a high-pressure center formed over the southeast of Brazil and persisted for 45 days, causing a hotter and drier summer than usual. The interaction of the high-level cyclonic vortex and the Bolivian high caused a confluence of the flow, favoring divergence at the surface (Fig. 2c, d). The South Atlantic high-pressure center was dislocated to the west (Fig. 2d), and the high-pressure center blocked the passage of CFs and the advection of moisture from the Amazon, preventing the formation of the South Atlantic convergence zone (Marengo et al., 2015).

This month presented the highest monthly average maximum temperature (31.7 °C), the highest temperature ever recorded (36.1 °C), the highest monthly average temperature (24.2 °C), the second-highest value of hours of clear skies (244.7 h, climatological mean is 151.1 h), and lower values of total precipitation (199.3 mm, climatological mean is 231.9 mm) at the IAG station, as compared to values from 1933 to 2014 (IAG-USP Meteorological Station, 2014). The UHI intensity, calculated using the surface meteorological station data, was also higher in 2014 than in other years (Ribeiro et al., 2015).

2.2. Numerical simulations

A series of numerical simulations were performed using the research version of the Weather Research and Forecasting model (Skamarock et al., 2008), Version 3.8.1, along with a single-layer urban canopy model (SLUCM; Chen et al., 2011). The SLUCM allows for three urban surface classes: low-density residential, high-density residential, and commercial/industrial. Hourly values of anthropogenic heat may be prescribed for each urban class. The classification of the MRSP urban area (Fig. 3) and the anthropogenic heat values used in this work are the same as those used by Ribeiro et al. (2018). Other parameterizations include: the Yonsei University planetary boundary layer (PBL) scheme was employed; the initial and boundary conditions for the outermost domain were obtained from the ERA-Interim reanalysis (Dee et al., 2011); the topography was obtained from the "Shuttle Radar Topography Mission" (Jarvis et al., 2008) satellite with three arc-second (approximately 90 m) resolution (Fig. 3a); ERA-Interim reanalysis data was used to update the sea surface temperature every six hours; the cumulus parameterization scheme was the Grell 3D ensemble; and the land surface scheme was Noah, with four soil layers. The outermost domain had 59 × 59 horizontal grid points with 9 km of grid space; the intermediate domain had 60 × 78 horizontal grid points, with 3 km of grid space; and the innermost domain had 66 × 108 horizontal grid points, with 1 km of grid space. In that regard, 38 vertical levels were used with the increasing grid space with height. The ratio between the spatial resolution of the initial and boundary conditions data (approximately 25 km) and that of the parent domain was similar to the ratio between domains (1/3). Validation data and additional details regarding the simulations may be found in Ribeiro et al. (2018).

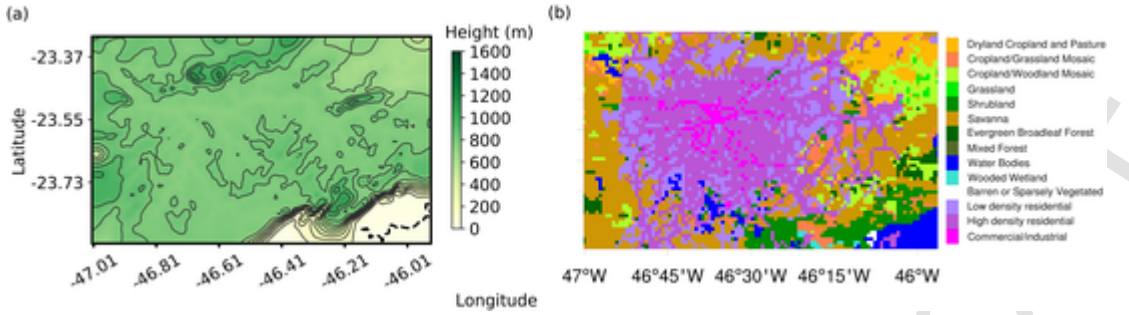

Fig. 3. Innermost domain (a) topography and (b) land use classes.

To determine the average pattern for the UHI in São Paulo during January, 10 simulations were performed, one for each year between 2004 and 2013. The simulations started at 2100 LT on December 31 of the previous year (00 Greenwich Mean Time) and ended at 0300 LT on February 01. However, only results from 0000 LT on January 1 to 0000 on February 01 were analyzed. Then, the near-surface (2 m) temperature fields for each daytime hour (from 0600 to 1800 LT) were separated from the nighttime hour fields (from 1900 to 0500 LT). To assess the spatial variability of the UHI, four rural points were determined at north, south, west, and east rural sites, and an urban point was determined at the city's most urbanized area (Fig. 1b). The UHI intensity was calculated as the temperature difference between the urban site and each rural site. The choice of the urban site was a point inside the area that presented higher values of air temperature at 2 m for all of the meteorological conditions. The rural sites were chosen by location, e.g., points that were not in an urban grid cell, and that presented an altitude similar to the city center point. There were not many choices for rural grid cells north and west of the city center with a similar altitude, as the terrain is higher in these areas (Fig. 3a).

The next step was to evaluate the meteorological conditions for each day. First, CF days were identified by analyzing synoptic reports from the Meteorological National Institute (INMET, http://www.inmet.gov.br/portal/ accessed on 03/18/2019). Then, the SB days were determined, using surface data from monitoring stations operated by the São Paulo State Environmental Company, and employing a methodology similar to the one used by Perez and Silva Dias (2017). In that regard, if the wind direction changed to SE during the day, the air temperature presented a decrease at the same hour, and there was not the influence of a CF, the day was marked as a SB day. As already noted by Perez and Silva Dias (2017), days that presented both CFs and SBs were considered only as CF days. Days that did not fall into the previous categories were considered no-front (NF) days. When a day was classified as SB, CF, or NF, all hourly results for that day (from 0000 to 2300 LT) were included in the corresponding average. The hourly averages of UHI intensity and the near-surface temperatures of daytime and nighttime fields were then calculated, considering all days, SB days, CF days, and NF days.

To assess the impact of the anomalous conditions during 2014 on UHI intensity, the simulation of this particular year and the averaging processes were performed as described above and were compared to the averages produced for the ten-year period.

3. Results

In this section, the average UHI pattern for the period from 2004 to 2013 is presented, and then the anomalous pattern in January of 2014 is compared to the average pattern.

3.1. Average urban heat island pattern

The analysis of the frequency of each meteorological condition for the ten months of January (2004–2013) resulted in an average occurrence of 38% of SB days, 35% of CF days, and 27% of NF days. These values varied from year to year: 2006 presented the highest frequency of SB passages (22 events), and 2013 presented the highest frequency of CF passages (19 events).

The effects of the different meteorological conditions (SB, CF, and NF) on the UHI hourly pattern are substantial, particularly for the daytime, as expected (Fig. 4). During the day, SB days show higher average temperatures, consistent with days with less cloudiness (Fig. 4a). The area with higher temperatures at the SE corner of the domain is the coast, and the contour lines NW from this area are related to the escarpment. The air cools as it flows up the escarpment during SB and CF days, forming an area of lower temperatures near the escarpment over the plateau. The UHI core (the area with higher temperatures) is displaced towards the NW. CF days show the lowest temperatures, as expected (Fig. 4b). For NF days, the UHI core is expanded towards the SE (Fig. 4c). As SB and CF days together represent more than 70% of the days, their impact is more evident on the all-days average (Fig. 4d). The topographic influence is also noticeable, not only near the escarpment, but also near the northern mountains and western higher-altitude areas that present lower temperatures.

During SB days, the predominant wind is from the NW, changing only during the passage of the SB front. SB passages impact the south part of the MRSP more frequently (Fig. 5g) and are hardly noticed in the north (Fig. 5a), where the SB flow is not intense enough to change the wind direction. At the center of the urban area (Fig. 5d), the east component of the wind evidences the SB

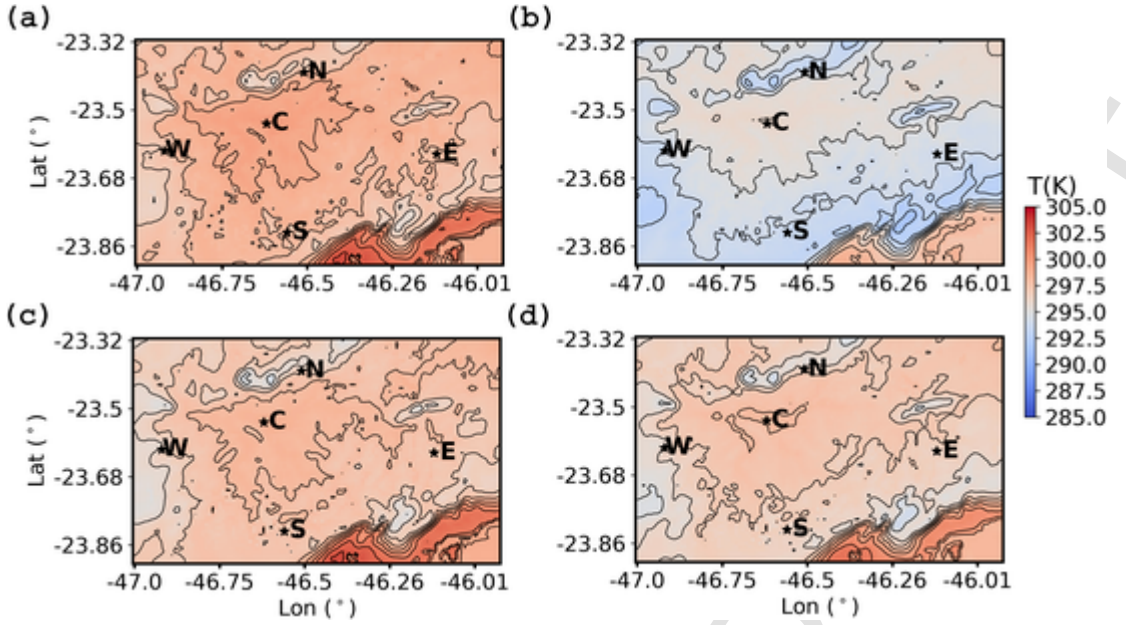

Fig. 4. Daytime (from 0600 to 1800 LT) air temperature average at 2 m in the innermost domain (a) for sea breeze, (b) cold front, (c) no-front, and (d) all days.

passage. The spatial difference in wind direction frequency is consistent with the converging pattern of UHI circulation already discussed by Ribeiro et al. (2018), and accelerates the SB propagation towards the center of the urban area (but decelerates this flow after the city center). NF days (Fig. 5b, e, h) show a much more frequent NW wind with higher speed that prevents the SB from propagating over the MRSP and are more spatially uniform than the other days. As this flow displaces the UHI core, it also displaces the UHI circulation, decreasing the SE flow frequency even in the south (Fig. 5h). CF days show a distinct pattern, with predominant wind direction between SE and E (Fig. 5c, f, i). This pattern brings colder air from the SE to the urban area, similar to SB days, but is a more persistent flow, and is more spatially uniform than for SB days.

NF nights present higher temperatures over rural areas, decreasing the UHI intensity as compared to SB nights (Fig. 6a,c). This occurs particularly over the southern and eastern rural areas and may be related to large-scale conditions that prevent the SB from reaching the plateau, and that brings continental air from the NW (Fig. 5h). The coast (SE corner of the innermost domain) has higher temperatures during SB and NF nights, as the predominant wind is from the NW (SB days may present a land breeze at night, see Fig. 5a, d, g), causing descending flows from the top of the escarpment to the coast, and increasing air temperature at lower altitudes. SB nights show a larger UHI core as compared to SB days. CF nights show a temperature field similar to that of CF days, with the UHI core advected to the NW (Fig. 6b) by the predominant flow (Fig. 5). On average, the nocturnal UHI is better-defined over the urban areas than the daytime UHI (Fig. 6d).

The UHI intensity during SB days shows the greatest value (4.5 °C) and variability (Fig. 7a). During the early morning, the UHI intensity decreases, as the air temperature in rural areas increases faster than in urban areas. Before noon, the UHI intensity starts increasing again, showing a maximum in the early evening, when the rural areas start cooling and the city still has stored heat. In the eastern and southern rural areas, there is a peak in UHI intensity at 1500 LT, probably caused by the passage of the SB front; at 1500 LT, the front has passed the southern and eastern rural areas, but not the city center. At 1600 LT, the front has passed the city center, decreasing the UHI intensity for the southern and eastern areas. Later, when the SB reaches the northern and western areas, the UHI intensity increases. As SBs are expected to occur more frequently in clear sky conditions, the greater values of UHI during the evening are probably related to heat storage in the urban canopy, to the incoming solar radiation during the day.

The CF days also show a different pattern for the eastern and southern rural areas as compared to the northern and western areas (Fig. 7b), as the CFs also arrive mainly from the SE, causing high UHI intensity values in the afternoon for the southern and eastern areas. The northern and western areas present lower UHI values during the day. Again, the higher values of UHI intensity occur during the early evening, when rural areas start cooling before urban areas. At night on CF days, the UHI intensity presents the lowest spatial variability, suggesting that CFs decrease the temperature variability over the region.

The NF days show the opposite pattern for the rural areas (Fig. 7c) as compared with the CF days, as the northern and western areas show higher UHI intensity during the afternoon than the eastern and southern areas. In these cases, the predominant direction of the wind is NW, bringing continental rural air to the NW vicinities of the city and urban air to the SE rural areas, and preventing cooler marine air from the SE from reaching the plateau. The UHI intensity values, except for in the western areas, are lower than those for the other meteorological conditions, particularly during the late evening. This suggests that the rural areas present higher temperatures on NF days. A topography contribution may occur, as air from the NW comes from higher ground and descends over the MRSP, increasing its temperature. The hourly average for all days (Fig. 7d) is composed of the contributions from the three situations, showing lower values during the morning and higher values in the afternoon and early evening, as in Ferreira et al. (2012)

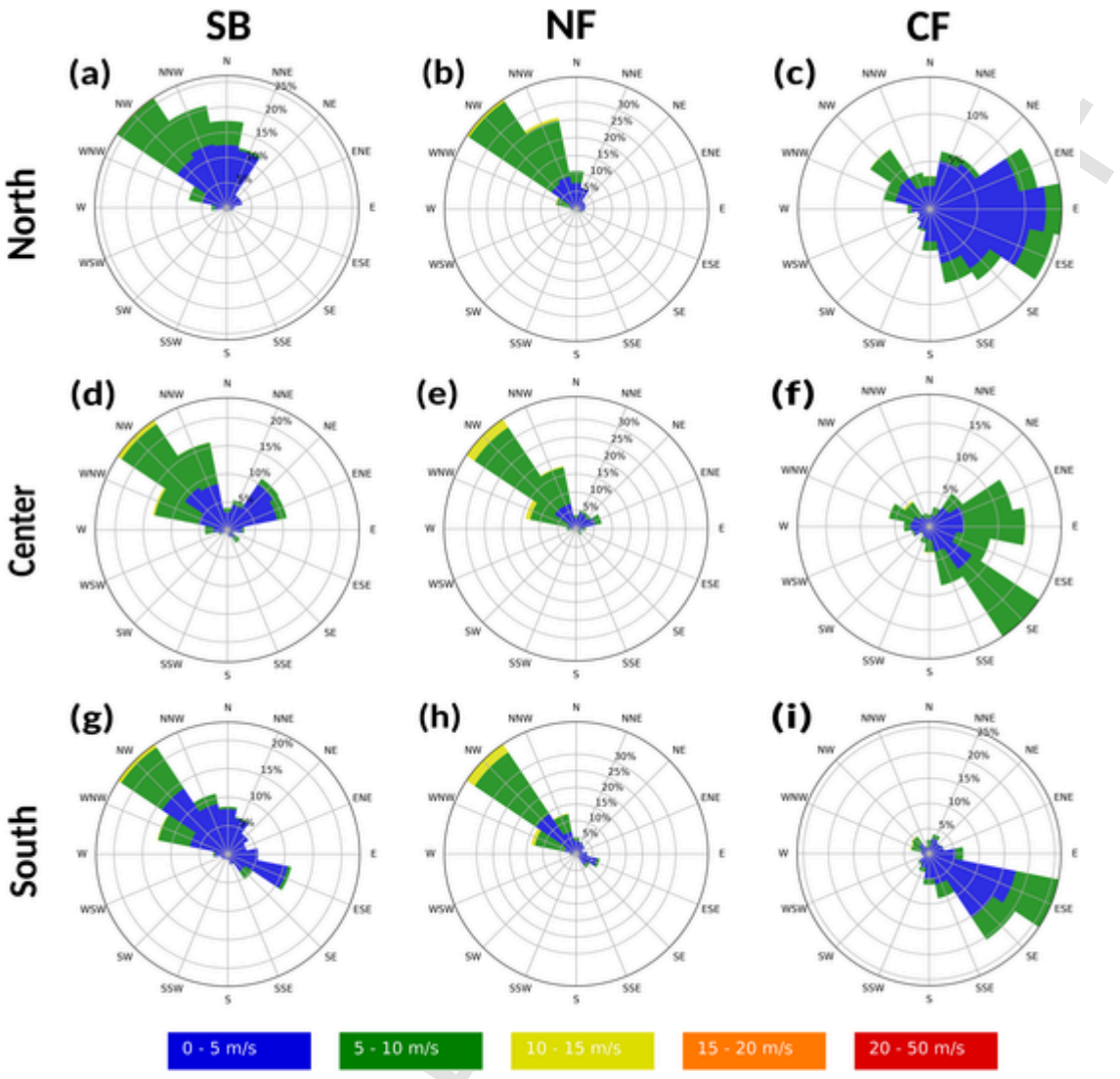

Fig. 5. Wind roses for (a), (b), (c) point N (North, Fig. 1), (d), (e), (f) point C (Center, Fig. 1), and (g), (h), (i) point S (South, Fig. 1) during sea breeze days (SB, a, d, g), no front days (NF, b, e, h), and cold front days (CF, c, f, i).

in 2004. As for other tropical cities (Chow and Roth, 2006; Li et al., 2013; Li and Norford, 2016; Murphy et al., 2011), the nighttime UHI intensity is higher than in the daytime.

3.2. January of 2014

In 2014, there were no CF passages, and there were 22 days with SBs (71% of the days of the month). Therefore, the all-day hourly averages of the UHI intensity for this year presented a SB pattern (dashed lines in Fig. 7a, d), with a sharp drop at 0700 LT and an increase from 0900 LT to the early evening. The UHI maximum intensity was higher than the average (from 1900 to 2000 LT, Fig. 7d), almost reaching 5.0 °C. In 2014, the SB days showed an increase in UHI intensity in comparison with the average, particularly in the southern area, from after 1800 LT to 0600 LT (Fig. 7a).

Nevertheless, the NF hourly pattern for 2014 (Fig. 7c) was very similar to the SB pattern for the same year (Fig. 7a). NF days presented a sharp decrease of UHI at 0700 LT, and then an increase (when considering northern and western rural areas) at 0900 LT (Fig. 7c). By comparing the eastern and southern areas, it is seen that the NF days presented an urban cold island between 0800 LT and 1200 LT. The prevailing NW wind that brought the continental rural air from the NW to the urban center increased the temperature difference between the NW rural areas and the UHI core. This flow also prevented SBs from propagating to the plateau, decreasing the temperature difference between the SE rural areas and the city. The difference between 2014 and the ten-year average for NF days seems also to be related to the prevailing clear sky conditions, giving NF days a similar pattern to SB days, but exchanging S and E areas with N and W areas.

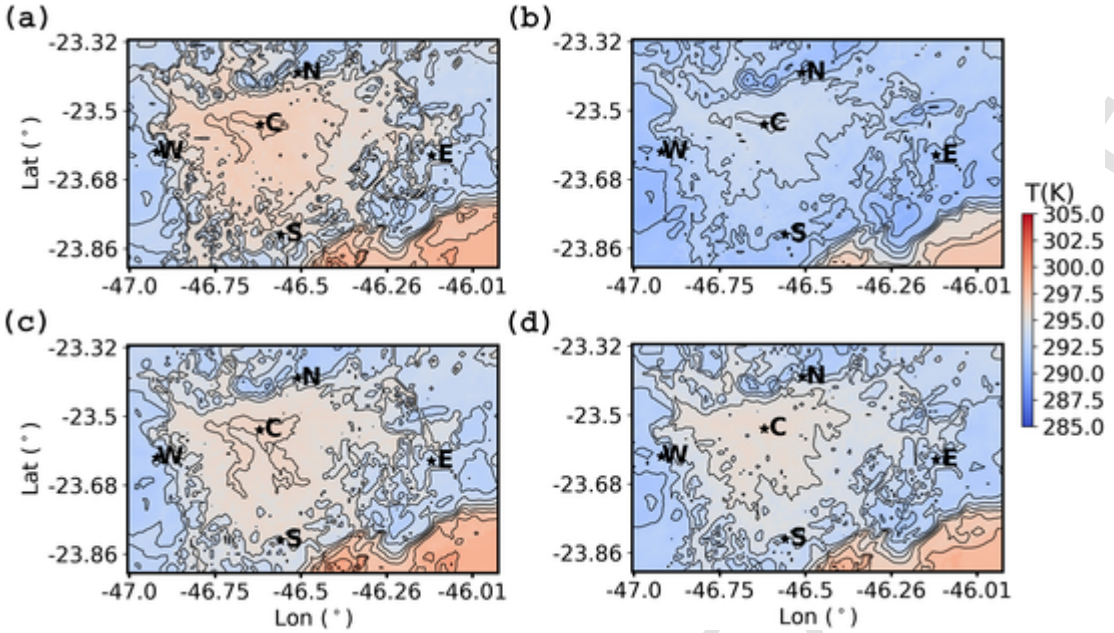

Fig. 6. Nighttime (from 1900 to 0500 LT) air temperature average at 2 m in the innermost domain (a) for sea breeze, (b) cold front, (c) no-front, and (d) all days.

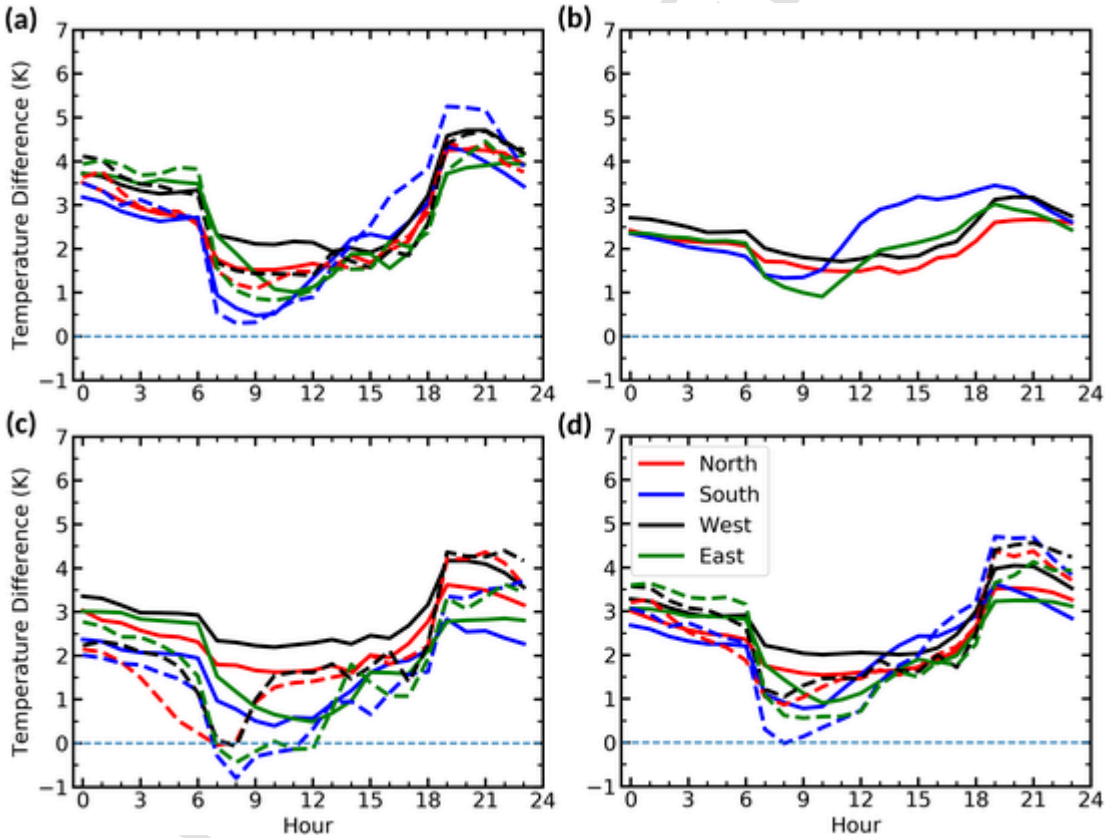

Fig. 7. Hourly averages of UHI intensity considering the northern (red line), the southern (blue line), the western (black line), and the eastern rural area (green line), for the ten year average (solid lines) and for 2014 (dashed lines) for (a) sea breeze, (b) cold front, (c) no-front, and (d) all days. (For interpretation of the references to colour in this figure legend, the reader is referred to the web version of this article.)

4. Conclusions

A numerical ten-year study of the UHI intensity in São Paulo during the month of January showed that the average values of UHI intensity varied from 1.5 to 2.5 K between 0000 LT and 1100 LT, and from 2.5 to 3.5 between 1200 LT and 2300 LT. The average UHI core (the urban area with higher air temperatures) was aligned in the SW-NE direction during the day. At night, the UHI core presented a more isotropic shape, and was more representative of the land use classification.

The UHI characteristics were also investigated under three distinct weather conditions: days that presented SB passages, days with CF passages, and days with NF passages. SB days presented the highest UHI intensity variability and the maximum values. This may be explained by the propagation of the SB front that, besides bringing cooler marine air, decreases the PBL height as observed by Ribeiro et al. (2018), thereby increasing the UHI intensity (Hidalgo et al., 2010). Additionally, calmer winds are related to higher UHI intensities (Yow, 2007), and SB days presented lower wind speeds overall (Fig. 5). Li et al. (2013) investigated the UHI intensity diurnal pattern during the intermonsoon season in Singapore along with the influence of SBs, and also found lower PBL heights caused by the SB passage. They found a UHI diurnal pattern similar to the one presented here: higher values during the night, and a sharp decrease in the early morning. The minimum and maximum values in São Paulo, however, were reached earlier, and the UHI maximum intensity was higher herein than for Singapore (5.5 °C vs. 2.4 °C, respectively). Murphy et al. (2011) investigated the UHI diurnal pattern for San Juan, Puerto Rico, and found the maximum UHI intensity just after sunrise (4.7 °C), particularly when comparing urban and forested areas, as forested areas took longer to initiate warming. Even though São Paulo is a coastal area, it is located at 700 m of altitude and has drier conditions than San Juan and Singapore; thus, the rural areas investigated here do not take as long after sunrise to begin warming.

The CF days present a less variable UHI intensity over the day, as CFs are large-scale phenomena that tend to overcome local circulations such as UHI. A CF also increases cloudiness and wind speed, conditions that are related to low UHI intensity (Yow, 2007). As the CF-predominant circulation is from the SE (Fig. 5), rural areas southeast from the urban area present higher UHI intensity than northwestern areas during the afternoon. NF days present higher variability in the UHI intensity as compared with CF days, but lower UHI values than SB days, as NF days are related to higher wind speeds than SB days, and lower cloudiness than CF days.

The large urban area and its topography increased the complexity in investigating the UHI patterns in São Paulo. Southeastern rural areas in the MRSP tend to be cooler than the other areas, owing to the influences of SB and CF propagation. The northern and western borders present rural areas in sites with slightly higher altitudes, where the topography presents a limit to urbanization. However, they are less frequently reached by SB fronts (Fig. 5). In NF days, the UHI core was larger, and the southern and eastern areas presented lower UHI intensities than northern and western areas for most of the day.

The nighttime UHI intensity was consistently higher for all meteorological conditions and areas, suggesting the important roles of impervious surfaces and heat storage in the urban canopy in maintaining higher air temperatures (Ryu and Baik, 2012), as the anthropogenic heat at night has low values in São Paulo (Ferreira et al., 2011). During the afternoon, the CF and SB days showed increased UHI intensity when comparing the urban temperatures with southern and eastern rural temperatures, and the NF days shows increased UHI intensity when comparing the urban temperatures with northern and western rural temperatures. Either way, the daytime UHI circulation is not symmetric when considering a NW-SE axis in the MRSP.

Other studies have examined the SB influences on the UHI intensity at the MRSP: Barros and Lombardo provided a picture of the surface UHI, and related it to vegetation; Silva et al. (2017) presented observational intra-urban temperature differences; Freitas et al. (2007) studied SB propagation during some days in winter, and the interactions with UHI; and Ribeiro et al. (2018) investigated the SB propagation impact on urban boundary layer development for one summer day and one winter day. However, these studies were only conducted only for certain days, and during particular atmospheric conditions. Here, a ten-year average for January was presented, producing a typical pattern for an austral summer day that may be used as reference for other studies aiming to study particular events, such as the atypical summer of 2014.

As compared to the ten-year average for January, January 2014 presented an hourly SB UHI intensity pattern, since as a high number of SB events occurred during this year in January. However, the same favorable conditions for SB propagation (low cloudiness and low wind speed) may also favor a more intense UHI (Yow, 2007). Therefore, the NF days in 2014 presented an hourly pattern similar to that of SB days, with differences caused by the prevailing NW wind. Additionally, the UHI intensity at night was higher in 2014 than the average of the previous ten years. Li and Bou-Zeid (2013) investigated the UHI intensity in Baltimore during a heat wave and found that the heat wave and the UHI interacted synergistically to increase heat stress, similar to what was observed in São Paulo in 2014. They developed an analytical model to determine the contributions of different processes in this interaction: energy availability differences between rural and urban sites, low wind speeds, and moisture availability differences. The authors also pointed out that, at night, the most important contributions are from differences in energy availability, as urban areas store more heat in their canopy than rural areas and release it at night. Therefore, it may be concluded that the major impact of the atypical weather conditions in 2014 was in the heat storage over the MRSP.

Declaration of Competing Interest

None

Acknowledgements

The authors thank the São Paulo Research Foundation (FAPESP), grants 2014/04372-2, 2017/20148-3, 2018/11217-4, and 2018/16478-0, for funding the research that supported this work.

References

Ackerman, B., 1985. Temporal march of the Chicago heat island. J. Clim. Appl. Meteorol. 24 (6), 547–554.
Barros, H.R., Lombardo, M.A., 2016. A ilha de calor urbana e o uso e cobertura do solo no município de São Paulo-SP. GEOUSP: Espaço e Tempo (Online) 20 (1), 160–177 (In Portuguese).
Bischoff-Gauß, I., Kalthoff, N., Fiedler, F., 1998. The impact of secondary flow systems on air pollution in the area of Sao Paulo. J. Appl. Meteorol. 37 (3), 269–287.
Chemel, C., Sokhi, R.S., 2012. Response of London's urban heat island to a marine air intrusion in an easterly wind regime. Bound.-Layer Meteorol. 144 (1), 65–81.
F. Chen H. Kusaka R. Bornstein J. Ching C. S. B. Grimmond S. Grossman-Clarke ... D. Sailor The integrated WRF/urban modelling system: development, evaluation, and applications to urban environmental problemsInternational Journal of Climatology3122011 273288
Chow, W.T., Roth, M., 2006. Temporal dynamics of the urban heat island of Singapore. Int. J. Climatol. 26 (15), 2243–2260.
de Coninck, H., Revi, A., Babiker, M., Bertoldi, P., Buckeridge, M., Cartwright, A., Dong, W., Ford, J., Fuss, S., Hourcade, J.-C., Ley, D., Mechler, R., Newman, P., Revokatova, A. Schultz, S., Steg, L. and Sugiyama, T., 2018. Strengthening and implementing the global response. In: Global Warming of 1.5°C. An IPCC Special Report on the Impacts of Global Warming of 1.5°C Above Pre-Industrial Levels and Related Global Greenhouse Gas Emission Pathways, in the Context of Strengthening the Global Response to the Threat of Climate Change, Sustainable Development, and Efforts to Eradicate Poverty Masson-Delmotte, V., P. Zhai, H.-O. Pörtner, D. Roberts, J. Skea, P.R. Shukla, A. Pirani, W. Moufouma-Okia, C. Péan, R. Pidcock, S. Connors, J.B.R. Matthews, Y. Chen, X. Zhou, M.I. Gomis, E. Lonnoy, T. Maycock, M. Tignor, and T. Waterfield (In Press).
D. P. Dee S. M. Uppala A. J. Simmons P. Berrisford P. Poli S. Kobayashi ... P. Bechtold The ERA-Interim reanalysis: Configuration and performance of the data assimilation systemQuarterly Journal of the royal meteorological society1376562011 553597
Dias, M.A.S., Machado, A.J., 1997. The role of local circulations in summertime convective development and nocturnal fog in São Paulo, Brazil. Bound.-Layer Meteorol. 82 (1), 135–157.
Ferreira, M.J., de Oliveira, A.P., Soares, J., 2011. Anthropogenic heat in the city of São Paulo, Brazil. Theor. Appl. Climatol. 104 (1–2), 43–56.
Ferreira, M.J., de Oliveira, A.P., Soares, J., Codato, G., Bárbaro, E.W., Escobedo, J.F., 2012. Radiation balance at the surface in the city of São Paulo, Brazil: diurnal and seasonal variations. Theor. Appl. Climatol. 107 (1–2), 229–246.
Freitas, E.D., Rozoff, C.M., Cotton, W.R., Dias, P.L.S., 2007. Interactions of an urban heat island and sea-breeze circulations during winter over the metropolitan area of São Paulo, Brazil. Bound.-Layer Meteorol. 122 (1), 43–65.
Grimmond, S.U.E., 2007. Urbanization and global environmental change: local effects of urban warming. Geogr. J. 173 (1), 83–88.
Harlan, S.L., Ruddell, D.M., 2011. Climate change and health in cities: impacts of heat and air pollution and potential co-benefits from mitigation and adaptation. Curr. Opin. Environ. Sustain. 3 (3), 126–134.
Hidalgo, J., Masson, V., Gimeno, L., 2010. Scaling the daytime urban heat island and urban-breeze circulation. J. Appl. Meteorol. Climatol. 49 (5), 889–901.
IAG-USP Meteorological Station Monthly Climatological Bulletin of the IAG/USP Meteorological Stationhttp://www.estacao.iag.usp.br/Mensais/Janeiro2014.pdf2014(Retrieved Apr 17, 2019 In Portuguese)
Jarvis, A., Reuter, H.I., Nelson, A., Guevara, E., 2008. Hole-Filled SRTM for the Globe Version 4. Accessed 9 December 2016. [available online at http://srtm.csi.cgiar.org from the CGIAR-CSI SRTM 90 m database.].
Keeler, J.M., Kristovich, D.A., 2012. Observations of urban heat island influence on lake-breeze frontal movement. J. Appl. Meteorol. Climatol. 51 (4), 702–710.
Kusaka, H., Kimura, F., Hirakuchi, H., Mizutori, M., 2000. The effects of land-use alteration on the sea breeze and daytime heat island in the Tokyo metropolitan area. J. Meteorol. Soc. Jpn. II 78 (4), 405–420.
Li, D., Bou-Zeid, E., 2013. Synergistic interactions between urban heat islands and heat waves: the impact in cities is larger than the sum of its parts. J. Appl. Meteorol. Climatol. 52 (9), 2051–2064.
Li, X.X., Norford, L.K., 2016. Evaluation of cool roof and vegetations in mitigating urban heat island in a tropical city, Singapore. Urban Clim. 16, 59–74.
Li, X.X., Koh, T.Y., Entekhabi, D., Roth, M., Panda, J., Norford, L.K., 2013. A multi-resolution ensemble study of a tropical urban environment and its interactions with the background regional atmosphere. J. Geophys. Res.-Atmos. 118 (17), 9804–9818.
J. A. Marengo C. A. Nobre M. E. Seluchi A. Cuartas L. M. Alves E. M. Mendiondo ... G. Sampaio A seca e a crise hídrica de 2014-2015 em São PauloRevista USP1062015 3144(In Portuguese)
Murphy, D.J., Hall, M.H., Hall, C.A., Heisler, G.M., Stehman, S.V., Anselmi-Molina, C., 2011. The relationship between land cover and the urban heat island in northeastern Puerto Rico. Int. J. Climatol. 31 (8), 1222–1239.
Oliveira, A.P., Bornstein, R.D., Soares, J., 2003. Annual and diurnal wind patterns in the city of São Paulo. Water, Air Soil Pollut. 3 (5–6), 3–15.
Perez, G.M., Silva Dias, M.A., 2017. Long-term study of the occurrence and time of passage of sea breeze in São Paulo, 1960–2009. Int. J. Climatol. 37, 1210–1220.
Ribeiro, F.N.D., Umezaki, A.S., Souza, J.F.T., Soares, J., Oliveira, A.P., Miranda, R.M., 2015. Urban heat island in the metropolitan area of São Paulo and the influence of warm and dry air masses during summer. In: 9th International Conference on Urban Climate jointly with 12th Symposium on the Urban Environment, 2015,Toulouse. http://www.meteo.fr/icuc9/LongAbstracts/ucp1-6-2241081_a.pdf.
Ribeiro, F.N., de Oliveira, A.P., Soares, J., de Miranda, R.M., Barlage, M., Chen, F., 2018. Effect of sea breeze propagation on the urban boundary layer of the metropolitan region of Sao Paulo, Brazil. Atmos. Res. 214, 174–188.
Ryu, Y.H., Baik, J.J., 2012. Quantitative analysis of factors contributing to urban heat island intensity. J. Appl. Meteorol. Climatol. 51 (5), 842–854.
Silva, F., Longo, K., de Andrade, F., 2017. Spatial and temporal variability patterns of the urban heat Island in São Paulo. Environments 4 (2), 27.
W. C. Skamarock J. B. Klemp J. Dudhia D. O. Gill D. M. Barker M. G. Duda ... J. G. Powers A description of the advanced research WRF version 3, NCAR Technical Note 2008 National Center for Atmospheric Research Boulder, CO, USA
Vemado, F., Pereira Filho, A.J., 2016. Severe weather caused by heat island and sea breeze effects in the metropolitan area of São Paulo, Brazil. In: Advances in Meteorology, 2016.
Yoshikado, H., 1992. Numerical study of the daytime urban effect and its interaction with the sea breeze. J. Appl. Meteorol. 31 (10), 1146–1164.
Yow, D.M., 2007. Urban heat islands: observations, impacts, and adaptation. Geogr. Compass 1 (6), 1227–1251.